 © 1981 The Chemical Society of Japan Bull. Chem. Soc. Jpn., 54, 901—908 (1981) 

# Phase Transition in Ammonium-$d_4$ Sulfate as Studied by Heat Capacity Measurements between 3 and 300 K†

Yoshiyuki HIGASHIGAKI†† and Hideaki CHIHARA*

*Department of Chemistry and Chemical Thermodynamics Laboratory, Faculty of Science, Osaka University, Toyonaka 560*

(Received September 17, 1980)

Molar heat capacities were determined of $(ND_4)_2SO_4$ between 2.8 and 301 K. The phase transition at 223.94±0.03 K is of the first-order with a long tail extending down to 160 K. The overall heat and entropy of transition are 4270 J mol$^{-1}$ and 20.35 J K$^{-1}$ mol$^{-1}$, respectively, the first-order portion contributing only 40%. The contraction of the molar volume at the transition was evaluated as 0.33 cm$^3$ mol$^{-1}$. The enthaply to misorient ions in an otherwise perfectly ordered lattice was derived from the low-temperature tail of the anomalous heat capacity. It was 12.0 kJ/mol of $(ND_4)_2SO_4$, in reasonable agreement with 16 kJ mol$^{-1}$ derived from O'Reilly-Tsang's mean field theory. The present results support the order-disorder mechanism of the transition.

Ammonium sulfate is probably one of the most extensively studied ferroelectric crystals. Its phase transition had been known to exist at about −50 °C by calorimetric investigations[1–3] before the ferroelectricity was discovered by Matthias and Remeika[4] in 1956. Since then reports have been published on its properties by such measurements as dielectric,[5,6] calorimetric,[5] X-ray[7] and electron[8] diffractions, neutron diffraction,[9] infrared[10,11] and far-infrared absorption,[12] neutron[13,14] and Raman[12] scattering, proton[10,15–18] and deuteron[17,19] magnetic resonance.

In spite of these studies, the nature of the phase transition has not been established; the neutron diffraction studies and the deuteron resonance studies gave conflicting interpretations. Thus, Schlemper and Hamilton[9] stated that both the high- and low-temperature phases were ordered from their neutron diffraction experiments on a single crystal of $(NH_4)_2SO_4$ whereas O'Reilly and Tsang[17] proposed that the transition is of an order-disorder type from their deuteron resonance. Both techniques indicate that there are two crystallographically inequivalent ammonium ions but the main issue is that whereas the neutron diffraction results can be interpreted by static distortion of the hydrogen-bonded ammonium tetrahedra, the deuteron resonance has to show a double minimum potential on each ammonium across the mirror plane in the high-temperature phase. O'Reilly and Tsang[20] then developed a molecular field theory based on a three-sublattice model involving disorder of sulfate ions. High resolution inelastic neutron scattering experiments[14] also support the dynamic order-disorder model.

More recently, an X-ray diffraction study[21] suggested strongly that the low-temperature phase of $(NH_4)_2SO_4$ was more properly described as a ferrielectric state in which the two types of inequivalent ammonium ions might assume separate order parameters. Peculiarity of the spontaneous polarization[26] at low temperatures and smallness of the Curie-Weiss constant in the high-temperature phase were also the reason to suspect the crystal to be ferrielectric at low temperatures.

Previous heat capacity results[2,5] are not sufficiently accurate for detailed examination of the transition; the measurements reported in this paper are consistent with the order-disorder model of the transition.

## Experimental

*Material.* Ammonium sulfate (Nakarai Chemicals, Ltd., stated purity better than 99.5%) was recrystallized from distilled water and dried in vacuo. Ammonium-$d_4$ sulfate was prepared by deuterium substitution of the recrystallized $(NH_4)_2SO_4$ in heavy water. Thus, the degassed heavy water with various deuterium concentrations (48.1—99.8%) was transfered onto solid in a vacuum apparatus to prevent pick-up of atmospheric water and then the aqueous solution was evaporated to dryness. The deuterium content of water which was distilled in vacuo was monitored with the integral proton intensity of the high resolution NMR at each substitution step. Water thus distilled at the final stage was found to have an isotopic purity of 99.6%. The $(ND_4)_2SO_4$ crystals thus obtained, however, showed a small thermal anomaly at about 250 K on DTA thermogram, which was likely to be due to $D_2O$ occluded in the $(ND_4)_2SO_4$ specimen. These crystals were then pulverized and heated to 80 °C under vacuum but this small DTA peak did not

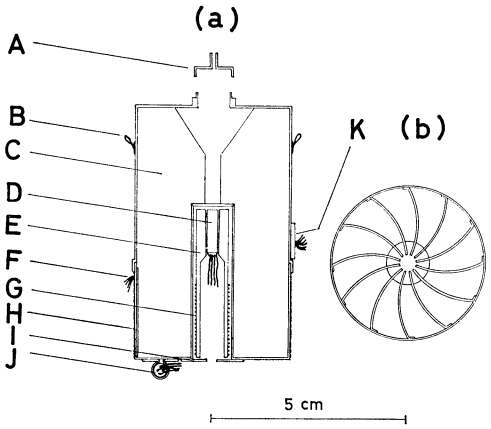


Fig. 1. Calorimeter vessel. (a) vertical cross-section (b) horizontal cross-section. A cap of vessel, B looped hook of copper, C gold-plated copper vane, D platinum thermometer, E thermometer/heater holder, F lead wire outlet, G KARMA heater, H lead wire wound non-inductively, I radiation trap, J germanium thermometer, K sleeve for differential thermocouples.

† Contribution No. 12 from Chemical Thermodynamics Laboratory, Faculty of Science, Osaka University.

†† Present address: Department of Chemistry, University of Utah, Salt Lake City, Utah 84112, U.S.A.

disappear completely. Therefore, the $(ND_4)_2SO_4$ crystals were dissolved in $D_2O$ again, recrystallized by slow cooling, separated from the solution by filtration, and dried *in vacuo*. Crystals thus prepared still showed a smaller heat anomaly at the same temperature as before, which disappeared after several thermal cycles between room temperature and liquid nitrogen temperature in a vacuum. Deuterium content of this sample was determined to be 99.3% from the deuterium content of the water distilled from the last mother liquor. Found: N, 19.90; S, 22.95%. Calcd for: N, 19.98; S, 22.87%.

The powder samples were put into the gold-plated copper calorimeter vessel which will be described below, in a conventional dry-box to reject atmospheric moisture. Weight of specimen used for calorimetry was 48.668 g (*in vacuo*), amounting to 0.34717 mol.

*Calorimeter and Cryostat.* The apparatus used was a newly constructed cryostat of a design similar to the one reported in the literature.[22] Some modifications were made to permit continuous operation from 2.5 K to 300 K using both liquid helium and liquid nitrogen. Once charged fully in the lower refrigerant tank, the liquid helium lasted for 6 to 10 h according as the upper tank contained solid nitrogen or solid hydrogen.

The calorimeter vessel is made of copper (0.3 mm in wall thickness) with 12 vertical vanes of copper (0.2 mm thick) as shown in Fig. 1. Both outside and inside were gold-plated. The platinum resistance thermometer D (Minco Products, Inc., Model S1055-1, Laboratory designation $\alpha$) was fitted to the copper holder E with soft solder around which the heater G (double-nylon insulated KARMA wire, Driver-Harris Co., B.S. #36) was wound non-inductively and fixed with G.E. 7031 adhesive. This thermometer/heater assembly was cast into the re-entrant well of the calorimeter vessel with Wood's alloy. Gold-plated radiation shield I covers most of the bottom to reduce direct heat exchange between the thermometer and the adiabatic shield that surrounds the calorimeter vessel. The germanium resistance thermometer J (CryoCal, Inc., Model CR 1000, Laboratory designation $\varepsilon$) was fitted into a copper sheath snugly with small amounts of silicone grease. The calorimeter vessel thus weighed 91 g including the attachments and its inside volume was 76 $cm^3$. In measurements of the heat capacity of the $(ND_4)_2SO_4$ sample, helium exchange gas less than $3.6\times10^{-5}$ mol was used for Series from I to XII and $1.5\times10^{-5}$ mol for Series from XIII to XV. Equilibration rates of the vessel containing $(ND_4)_2SO_4$ varied greatly. At temperatures below 20 K, the sample reached equilibrium in ten seconds to a few minutes. At higher temperatures it took about 15 min for equilibrium, except near the ferroelectric transition temperature where it was much longer. The sample contributed 23% to the total heat capacity at 3 K: the contribution increased to more than 60% above 100 K.

*Temperature Scales.* The platinum thermometer ($\alpha$) was used above 14 K and the germanium thermometer ($\varepsilon$) below 15 K. They were calibrated prior to the measurements of heat capacity.

The temperature scale of the thermometer $\alpha$ was fixed based on the 1968 International Practical Temperature Scale (IPTS 68). The necessary resistance values at the eight defining fixed points from 13.81 to 373.15 K were obtained by comparison with the Leeds & Northrup platinum thermometer (Model 8164) whose scale was determined at the U.S. National Bureau of Standards on IPTS 68. The thermometer $\alpha$ proved to satisfy the condition for the SPRT; $R(100\ °C)/R(0\ °C)\geqq1.3925$. The necessary coefficients for the IPTS 68 scale below 0 °C were calculated according to the standard procedure.[23] To obtain the scale between 0 and 100 °C, the resistance values were measured from 255 to 380 K at intervals of 5 K instead of determining the value at the freezing point of tin or zinc. Observed values of temperatures based on the IPTS 68 and the resistances were fitted to the following empirical formula;

$$R(t) = R(0)\{1+A\,t+B\,t^2+C(t-100)t^3\},$$

where $t=T_{68}-273.15$.

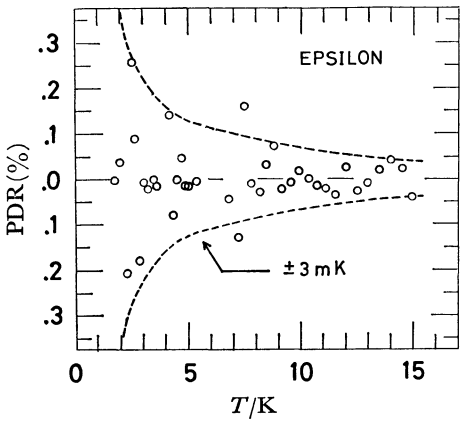


Fig. 2. Percent deviation (PDR) of calibration points from the smooth values of the germanium temperature scale.

The germanium thermometer $\varepsilon$ was compared with the germanium thermometer (the same model, laboratory designation $\gamma$) which had been calibrated in our laboratory using the helium vapor pressures and gas thermometry on the IPTS 68. Resistance value of the thermometer $\varepsilon$ was about 1 kΩ at 4.2 K and the calibration current of 5.7 μA was chosen to avoid the adverse effect of self-heating. To obtain the interpolation formula, a series expansion of the type

$$\log R = \sum_i A_i(\log T)^{k+i}$$

was used to fit the calibration data. The variance $V$ given by

$$(M-1)V^2 = \sum_{j=1}^{M}\{R_j(\text{observed})-R_j(\text{smoothed})\}^2,$$

where $M$ (=38) is the number of calibration points, and the temperature dependences of the first and second derivatives of log $R$ with respect to log $T$ were employed as a measure of fitting. The best fit was obtained when the power $k+i$ of the first term was taken as −2 and the number of the series expansion terms as 10. The temperature determined by the thermometer $\varepsilon$ deviated less than 5 mK from the thermodynamic temperature between 1.8 and 15 K as shown in Fig. 2.

## Results and Discussion

The experimental molar heat capacity is given in Table 1 in chronological sequence at the mean temperatures of determination. The temperature increment in each measurement was small as seen from the differences in the adjacent mean temperatures and hence no curvature correction was made. Corrections were not made either for the contribution from the helium exchange gas in calculating the heat capacity values because of negligible contribution. Scattering

TABLE 1. MOLAR HEAT CAPACITIES OF $(ND_4)_2SO_4$
Weight of specimen 48.668 g. Molecular weight 140.18. IPTS-68.

| $T$/K | $C_p$/J K$^{-1}$ mol$^{-1}$ | $T$/K | $C_p$/J K$^{-1}$ mol$^{-1}$ | $T$/K | $C_p$/J K$^{-1}$ mol$^{-1}$ | $T$/K | $C_p$/J K$^{-1}$ mol$^{-1}$ | $T$/K | $C_p$/J K$^{-1}$ mol$^{-1}$ |
|---|---|---|---|---|---|---|---|---|---|
| Series I | | 158.533 | 142.34 | 222.842 | 304.90 | 217.347 | 250.33 | 49.969 | 36.92 |
| 58.928 | 47.25 | 160.864 | 144.48 | 223.675 | 939.0 | 218.696 | 259.07 | 51.380 | 38.52 |
| 60.517 | 49.09 | 163.162 | 146.75 | 223.934 | 17323 | 220.010 | 269.11 | 52.738 | 40.08 |
| 62.272 | 51.04 | 165.438 | 149.03 | 223.973 | 11975 | 221.282 | 281.20 | 54.058 | 41.54 |
| 64.032 | 53.09 | 167.696 | 151.32 | 224.291 | 704.52 | 222.502 | 297.61 | 55.344 | 43.07 |
| 65.698 | 54.97 | 169.437 | 153.72 | 225.365 | 177.25 | 223.499 | 482.00 | 56.600 | 44.50 |
| 67.403 | 56.85 | 172.152 | 155.84 | 227.013 | 175.99 | 223.921 | 12020 | 57.940 | 46.06 |
| 69.071 | 58.82 | Series III | | Series V | | 223.956 | 14578 | 59.351 | 47.68 |
| 70.609 | 60.50 | 161.730 | 144.67 | (Transition region, | | 223.998 | 8796.6 | Series XIII | |
| 72.192 | 62.19 | 163.626 | 146.68 | run 2. continuous | | 224.539 | 356.40 | 3.121 | 0.0121 |
| 73.746 | 63.87 | 165.597 | 148.74 | heating) | | 225.922 | 175.58 | 3.546 | 0.0193 |
| 75.274 | 65.57 | 167.634 | 150.88 | Series VI | | 227.655 | 175.74 | 3.988 | 0.0270 |
| 77.041 | 67.49 | 169.640 | 152.89 | 226.035 | 175.34 | 229.387 | 175.90 | 4.411 | 0.0401 |
| 78.705 | 69.34 | 171.618 | 155.24 | 227.674 | 175.31 | Series IX | | 4.807 | 0.0504 |
| 80.170 | 70.88 | 173.571 | 157.23 | 229.314 | 175.89 | (Transition region, | | 5.183 | 0.0625 |
| 81.710 | 72.74 | 175.496 | 159.48 | 230.872 | 175.90 | run 3 and 4. conti- | | 5.571 | 0.0798 |
| 83.310 | 74.17 | 177.392 | 161.81 | 232.503 | 176.53 | nuous heating) | | Series XIV | |
| 85.039 | 76.03 | 179.268 | 163.90 | 234.210 | 176.71 | Series X | | 2.814 | 0.0083 |
| 86.765 | 77.82 | 181.110 | 165.88 | 235.985 | 176.78 | 14.104 | 1.839 | 3.117 | 0.0113 |
| 88.435 | 79.45 | 182.939 | 168.13 | 237.827 | 177.47 | 15.134 | 2.313 | 3.439 | 0.0167 |
| 90.147 | 81.13 | 184.748 | 170.72 | 239.670 | 177.90 | 16.220 | 2.885 | 3.756 | 0.0221 |
| 91.910 | 82.97 | 186.530 | 173.30 | 241.517 | 178.71 | 17.664 | 3.784 | 4.066 | 0.0294 |
| 93.689 | 84.96 | 188.293 | 175.73 | 243.450 | 179.44 | 20.500 | 5.903 | 4.368 | 0.0348 |
| 95.464 | 86.43 | 190.117 | 178.43 | 245.456 | 179.51 | 23.827 | 8.765 | 4.692 | 0.0450 |
| 97.234 | 88.09 | 191.999 | 181.54 | 247.394 | 180.36 | Series XI | | 5.005 | 0.0547 |
| 99.020 | 89.76 | 193.861 | 184.63 | 249.345 | 180.83 | 14.033 | 1.806 | 5.334 | 0.0725 |
| 100.823 | 91.51 | 195.692 | 188.33 | 251.436 | 181.59 | 14.927 | 2.201 | 5.669 | 0.0847 |
| 102.703 | 93.18 | 197.494 | 191.16 | Series VII | | 16.724 | 3.184 | 6.064 | 0.1014 |
| 104.572 | 95.04 | 199.285 | 194.80 | 251.347 | 181.54 | 17.722 | 3.818 | 6.502 | 0.1260 |
| 106.456 | 96.64 | 201.062 | 198.68 | 253.364 | 182.32 | 18.911 | 4.646 | 7.003 | 0.1567 |
| Series II | | 202.812 | 202.79 | 255.769 | 182.99 | 20.191 | 5.619 | 7.579 | 0.2014 |
| 106.111 | 96.31 | 204.535 | 207.06 | 258.315 | 183.76 | 21.398 | 6.593 | 8.307 | 0.2747 |
| 107.979 | 97.98 | 206.229 | 211.27 | 260.849 | 184.54 | 22.526 | 7.559 | 9.179 | 0.3905 |
| 107.848 | 99.63 | 207.882 | 214.99 | 263.129 | 185.00 | 23.604 | 8.522 | 10.203 | 0.5751 |
| 111.738 | 101.34 | 209.515 | 219.23 | 265.391 | 186.08 | Series XII | | 11.374 | 0.8543 |
| 113.643 | 103.20 | 211.123 | 224.11 | 267.893 | 187.13 | 24.117 | 9.017 | 12.523 | 1.191 |
| 115.560 | 104.54 | 212.699 | 229.43 | 270.474 | 187.74 | 25.106 | 9.949 | 13.637 | 1.605 |
| 117.493 | 106.33 | 214.247 | 234.81 | 273.136 | 188.73 | 26.086 | 10.90 | Series XV | |
| 119.437 | 108.07 | 215.832 | 239.68 | 275.800 | 189.40 | 27.166 | 11.94 | 3.948 | 0.0253 |
| 121.401 | 109.77 | 217.381 | 249.53 | 278.443 | 190.13 | 28.325 | 13.05 | 4.237 | 0.0346 |
| 123.386 | 111.16 | Series IV | | 281.145 | 191.71 | 29.299 | 14.02 | 4.521 | 0.0422 |
| 125.397 | 113.70 | (Transition region, | | 283.912 | 192.02 | 30.243 | 15.02 | 4.812 | 0.0535 |
| 127.429 | 114.96 | | run 1) | 286.676 | 193.05 | 31.299 | 16.11 | 5.192 | 0.0699 |
| 129.478 | 116.96 | 204.289 | 205.81 | 289.426 | 193.96 | 32.453 | 17.25 | 5.675 | 0.0850 |
| 131.546 | 118.66 | 205.812 | 209.74 | 292.244 | 194.77 | 33.698 | 18.47 | 6.194 | 0.1081 |
| 133.610 | 120.52 | 207.387 | 214.12 | 295.120 | 195.62 | 34.990 | 20.20 | 6.765 | 0.1405 |
| 136.073 | 122.61 | 208.939 | 218.56 | 298.051 | 196.67 | 36.283 | 21.78 | 7.392 | 0.1855 |
| 138.614 | 124.75 | 210.466 | 222.70 | 301.049 | 197.74 | 37.493 | 23.21 | 8.165 | 0.2592 |
| 140.823 | 126.89 | 211.959 | 227.18 | Series VIII | | 38.694 | 24.48 | 9.015 | 0.3683 |
| 142.997 | 128.65 | 213.422 | 233.37 | (Transition region, | | 40.063 | 25.89 | 9.910 | 0.5179 |
| 145.136 | 130.53 | 214.928 | 238.64 | | run 3) | 41.536 | 27.45 | 10.841 | 0.7174 |
| 147.530 | 132.60 | 216·397 | 247.09 | 210.335 | 223.03 | 42.917 | 28.45 | 11.747 | 0.9549 |
| 149.855 | 134.50 | 217.766 | 254.84 | 211.674 | 227.11 | 44.259 | 30.44 | 12.605 | 1.217 |
| 151.916 | 136.22 | 219.097 | 262.68 | 213.135 | 232.13 | 45.608 | 31.95 | 13.461 | 1.526 |
| 154.054 | 138.12 | 220.391 | 273.24 | 214.564 | 238.37 | 47.005 | 33.49 | 14.362 | 1.938 |
| 156.257 | 140.10 | 221.642 | 286.11 | 215.965 | 242.98 | 48.487 | 35.20 | | |

TABLE 2. THERMODYNAMIC FUNCTIONS OF $(ND_4)_2SO_4$ TO 300 K

| $T$ / K | $C_p°$ / J K$^{-1}$ mol$^{-1}$ | $S°$ / J K$^{-1}$ mol$^{-1}$ | $(H_T°-H_0°)T^{-1}$ / J K$^{-1}$ mol$^{-1}$ | $-(G_T-H_0°)T^{-1}$ / J K$^{-1}$ mol$^{-1}$ |
|---|---|---|---|---|
| 5 | 0.0546 | 0.0180 | 0.0135 | 0.0045 |
| 10 | 0.5353 | 0.1584 | 0.1208 | 0.0376 |
| 15 | 2.233 | 0.6456 | 0.4999 | 0.1457 |
| 20 | 5.467 | 1.695 | 1.308 | 0.3871 |
| 25 | 9.833 | 3.367 | 2.561 | 0.8061 |
| 30 | 14.75 | 5.589 | 4.178 | 1.411 |
| 35 | 20.14 | 8.261 | 6.068 | 2.193 |
| 40 | 25.69 | 11.31 | 8.174 | 3.139 |
| 45 | 31.22 | 14.66 | 10.43 | 4.230 |
| 50 | 36.79 | 18.23 | 12.78 | 5.450 |
| 60 | 48.26 | 25.95 | 17.73 | 8.213 |
| 70 | 59.76 | 34.27 | 22.94 | 11.34 |
| 80 | 70.77 | 42.98 | 28.23 | 14.74 |
| 90 | 81.08 | 51.91 | 33.54 | 18.38 |
| 100 | 90.75 | 60.96 | 38.78 | 22.18 |
| 110 | 99.86 | 70.04 | 43.92 | 26.12 |
| 120 | 108.61 | 79.11 | 48.95 | 30.16 |
| 130 | 117.30 | 88.14 | 53.87 | 34.27 |
| 140 | 126.01 | 97.16 | 58.72 | 38.44 |
| 150 | 134.52 | 106.14 | 63.49 | 42.65 |
| 160 | 143.59 | 115.11 | 68.20 | 46.90 |
| 170 | 153.60 | 124.11 | 72.93 | 51.18 |
| 180 | 164.76 | 133.20 | 77.72 | 55.48 |
| 190 | 178.29 | 142.45 | 82.64 | 59.81 |
| 200 | 196.49 | 152.03 | 87.85 | 64.18 |
| 210 | 221.0 | 162.18 | 93.58 | 68.61 |
| 220 | 269.1 | 173.38 | 100.27 | 73.11 |
| 230 | 175.8 | 190.67 | 112.76 | 77.91 |
| 240 | 178.0 | 198.19 | 115.43 | 82.76 |
| 250 | 181.1 | 205.52 | 117.99 | 87.53 |
| 260 | 184.4 | 212.69 | 120.49 | 92.20 |
| 270 | 187.6 | 219.71 | 122.91 | 96.80 |
| 280 | 190.8 | 226.59 | 125.28 | 101.31 |
| 290 | 194.0 | 233.34 | 127.59 | 105.75 |
| 300 | 197.3 | 239.97 | 129.86 | 110.11 |
| 273.15 | 188.5 | 221.88 | 123.66 | 98.22 |
| 298.15 | 196.6 | 238.74 | 129.44 | 109.30 |

of results was within 15% below 8 K, decreasing to 2% between 8 and 15 K, within 1% between 15 and 50 K, and 0.5% above 50 K. When our results are compared with the data by Nitta and Suenaga,[2] their values are found systematically larger than ours by 13% in the low-temperature phase and by 8% in the high-temperature phase. Hoshino *et al.*[5] also reports values too large by 24% at 200 K and 15% at 250 K in a similar manner to the case of $NH_4HSO_4$.[24] The entire heat capacity curve is shown in Fig. 3.

The thermodynamic functions were evaluated from the smoothed values of the heat capacity and are summarized in Table 2 at rounded temperatures, including the contributions from the heat capacity below 3 K and near the transition region which will be discussed later.

*Low Temperature Heat Capacity.* From the $C_pT^{-3}$ *versus* $T^2$ plot, the heat capacity values below 5 K were estimated by using the formula,

$$10^4\, C_pT^{-3} = 4.28 \pm 0.04 + 0.003\, T^2,$$

where $C_p$ is in the units of J K$^{-1}$ mol$^{-1}$ and the coefficient of the second term has an uncertainty of about 20%. This coefficient is smaller by a factor of 25 than that of $(NH_4)_2SO_4$ for which it is 0.08. The Debye temperature at 0 K was found to be 238.8±0.7 K for $9N$ degrees of freedom and 165.6±0.5 K for $3N$ degrees of freedom.

*'Normal' Behavior.* We now attempt to separate the 'normal' portion of the observed heat capacity in order to assess the 'abnormal' portion associated with the phase transition and to see to what extent the normal portion may be rationalized in terms of harmonic vibrational spectrum. The best practical way in which to find the temperature at which the abnormal contribution begins to be seen is to plot the equivalent Debye temperature $\theta_D$ as a function of temperature (see Fig. 4) and then draw a smooth curve ignoring the transition region. The normal por-

Table 3. Estimated normal heat capacities of $(ND_4)_2SO_4$ at rounded temperatures

| $T$/K | $C_p$/J K$^{-1}$ mol$^{-1}$ | $T$/K | $C_p$/J K$^{-1}$ mol$^{-1}$ | $T$/K | $C_p$/J K$^{-1}$ mol$^{-1}$ | $T$/K | $C_p$/J K$^{-1}$ mol$^{-1}$ |
|---|---|---|---|---|---|---|---|
| 95 | 85.9 | 150 | 130.4 | 205 | 161.4 | 260 | 184.0 |
| 100 | 90.7 | 155 | 133.7 | 210 | 163.7 | 265 | 185.8 |
| 105 | 95.4 | 160 | 136.9 | 215 | 165.9 | 270 | 187.5 |
| 110 | 99.9 | 165 | 140.0 | 220 | 168.1 | 275 | 189.2 |
| 115 | 104.3 | 170 | 143.0 | 225 | 170.2 | 280 | 190.9 |
| 120 | 108.5 | 175 | 145.9 | 230 | 172.3 | 285 | 192.5 |
| 125 | 112.4 | 180 | 148.7 | 235 | 174.3 | 290 | 194.0 |
| 130 | 116.2 | 185 | 151.4 | 240 | 176.3 | 295 | 195.5 |
| 135 | 119.9 | 190 | 154.0 | 245 | 178.3 | 300 | 197.0 |
| 140 | 123.5 | 195 | 156.5 | 250 | 180.2 | 305 | 198.3 |
| 145 | 127.0 | 200 | 159.0 | 255 | 182.1 | 310 | 199.7 |

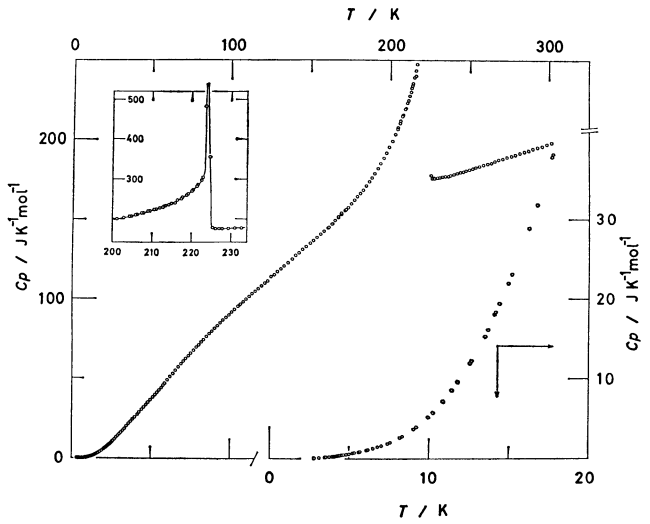


Fig. 3. Measured heat capacities of $(ND_4)_2SO_4$.

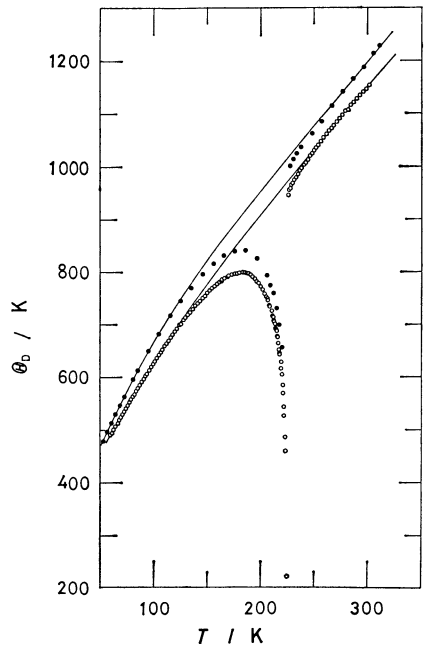


Fig. 4. Assessment of 'normal' heat capacities by the use of Debye temperature $\theta_D$. Open circles for $(ND_4)_2SO_4$ and filled circles for $(NH_4)_2SO_4$.

tion of the heat capacity thus obtained is given in Table 3.

We may divide a total of $45N$ degrees of freedom into the $9N$ lattice vibrational modes, $3N$ librational modes of $SO_4^{2-}$, $6N$ librational modes of $ND_4^+$, $9N$ internal modes of $SO_4^{2-}$ and 18 internal modes of $ND_4^+$, assuming that the intermolecular interactions are much weaker than the intramolecular interaction. The lattice vibrational contributions to the normal heat capacity may be derived from a Debye function with $\theta_D(0\,K)=238$ K. Other contributions can be estimated from the fundamental frequencies observed in the infrared and far infrared absorption spectra and also the Raman scattering; that is, for $ND_4^+$, $\nu_1(A_1)=2220$, $\nu_2(E)=1215$, $\nu_3(F_2)=2390$, $\nu_4(F_2)=1032$, $\nu_L=260$ and for $SO_4^{2-}$, $\nu_1(A_1)=973$, $\nu_2(E)=452$ and 464, $\nu_3(F_2)=1110$, $\nu_4(F_2)=614$ and 626, $\nu_L=102$ and 130 in units of cm$^{-1}$. Assuming that the librational modes of cations and anions are dispersion-less, the sum total of their modes accounts for most of the normal heat capacity above 120 K. However, such estimation exceeds the observed by about 10 J K$^{-1}$ mol$^{-1}$ at 80 K, which is outside of the experimental error. The anharmonic effects are usually too small to be seen at this temperature and, therefore, the discrepancy probably comes from inadequacy of the Debye approximation for the $9N$ degrees of freedom. The $9N$ degrees of 'lattice' freedom can further be divided into $3N$ acoustic modes and $6N$ optical modes. Since the translational optical mode frequencies are nearly independent of their wave vectors, compared with the acoustic modes, we tried to fix the average frequency of these optical modes by means of an Einstein function. As to the acoustic modes the value of $\theta_D(0\,K)=165.6$ K was used in the Debye approximation for $3N$ degrees of freedom. The best fit was obtained when the average optical frequency was chosen to be $185\pm5$ cm$^{-1}$. This value is consistent with the broad far infrared bands centering at 180 and 200 cm$^{-1}$ which are assigned as the translational modes of $ND_4^+$ by our preliminary study[25] shown in Fig. 5. This value also shows a good agreement with the broad peak at $200\pm16$ cm$^{-1}$ in the neutron inelastic scattering experiment,[13] the assignment of which is

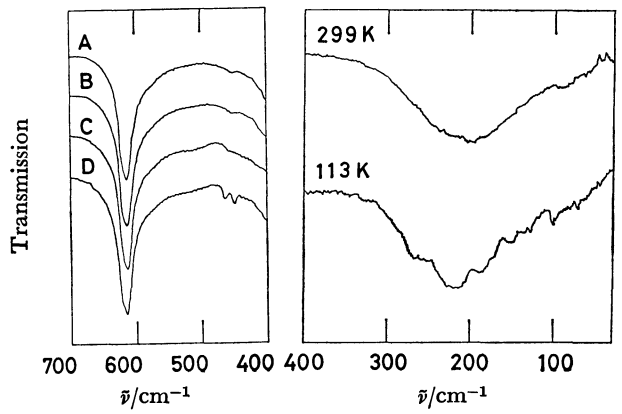


Fig. 5. Infrared and far infrared spectra of $(ND_4)_2SO_4$.

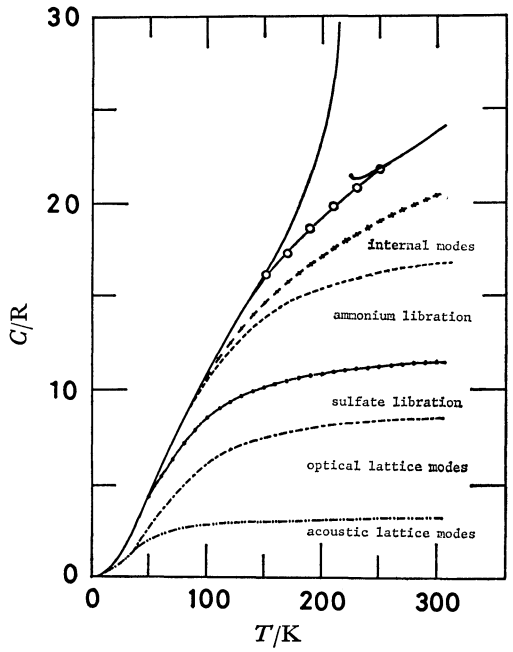


Fig. 6. Breakdown of the normal heat capacity into contributions.

the same as ours. Figure 6 shows the final result of the present analysis on the normal heat capacity of $(ND_4)_2SO_4$. Remaining discrepancy of about 10% of the normal $C_p$ value at 200 K (14% at 300 K) is partly due to neglected $C_p$-$C_V$ correction and partly due to the onset of anharmonic effects.

*Ferroelectric (Ferrielectric) Phase Transition.* The transition temperature of $(ND_4)_2SO_4$ was determined from the position of maximum heat capacity as 223.94± 0.03 K and is compared with previous determinations and with the results for $(NH_4)_2SO_4$ in Table 4. There is virtually no effect of deuterium substitution on the transition temperature. This fact indicates that the Gibbs energies on both sides of the transition change by the same magnitude upon deuteration. Because the modes of motion that suffer from the largest influence are those related to libration of ammonium ions, the potential energy surface which an ammonium ion sees when it rotates changes little on passing through the transition. In other words, there is little difference in the libration frequency between the low- and high-

TABLE 4. TRANSITION TEMPERATURES OF $(NH_4)_2SO_4$ AND $(ND_4)_2SO_4$

| $T_c$/K of $(NH_4)_2SO_4$ | $T_c$/K of $(ND_4)_2SO_4$ |
|---|---|
| 223.1[a] | 223.6[a] |
| 223.4[b] | |
| 223.0[c] | 223.7[c] |
| 225.7[c] | 225.2[c] |
| | 223.94±0.03[d] |

a) Ref. 2. b) Ref. 3. c) Ref. 5. d) Present research.

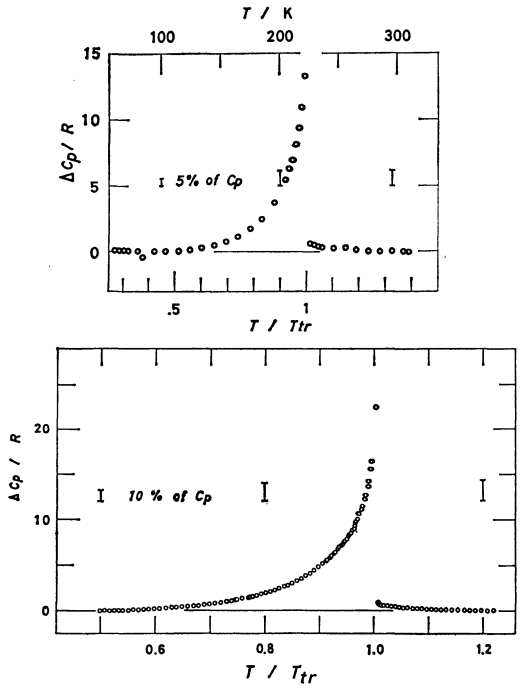


Fig. 7. Anomalous part of heat capacity. Top $(NH_4)_2SO_4$, Bottom $(ND_4)_2SO_4$.

temperature phases. This is consistent with the fact it was possible to draw a continuous smooth curve between the normal portions on the $\theta_D$ *vs.* $T$ plot (Fig. 4). This also leads to an important notion that the transition mechanism can not be such as to accompany a substantial change in the librational state of the ammonium ions. If the ammonium ions are to play a leading role in the transition, it will be either order-disorder between almost equivalent orientations or translational displacement.

The transition is of first order with a long tail on the low-temperature side (down to $0.6T_c$). Other properties also show the first-order characteristics, like thermal hysteresis,[2] molar volume,[5] spin-lattice relaxation time of NMR,[17,19] and spontaneous polarization.[5] The present calorimetric study showed that the time for equilibration was extremely long in the transition region, as long as three hours. However, the latent heat and its corresponding entropy change account for only 40% of the overall heat and entropy of the transition (1.8 kJ mol$^{-1}$ and 8.1 J K$^{-1}$ mol$^{-1}$). The overall shape of the heat capacity anomaly is shown in Fig. 7. The inset of Fig. 3 depicts how the latent heat portion begins abruptly after very gradual rise of the heat capacity. The temperature

Table 5. Enthalpy and entropy of transition in $(NH_4)_2SO_4$ and $(ND_4)_2SO_4$

| $(NH_4)_2SO_4$ | | $(ND_4)_2SO_4$ | |
|---|---|---|---|
| $\Delta H_c$ / J mol$^{-1}$ | $\Delta S_c$ / J K$^{-1}$ mol$^{-1}$ | $\Delta H_c$ / J mol$^{-1}$ | $\Delta S_c$ / J K$^{-1}$ mol$^{-1}$ |
| 3890[a] | 18[a] | 3890[a] | 18[a] |
| — | 16.7[b] | 4270[c] | 20.35[c] |

a) Ref. 5. b) Ref. 3. c) Present research.

dependence between $0.6T_c$ and $T_c$ is very much like that of dielectric anomaly[5,6]. Table 5 lists the thermodynamic quantities of the transition in comparison with corresponding results for $(NH_4)_2SO_4$. These are large, perhaps one of the largest among the ferroelectric transitions. Shomate[3] reported a value of 16.7 J K$^{-1}$ mol$^{-1}$ for the 'excess' entropy of $(NH_4)_2SO_4$ which is smaller than our value of 20.4 for $(ND_4)_2SO_4$ by as much as 18%. His value is based on an arbitrary assessment of the 'normal' curve and it is not possible to deduce from his published primary results a quantity which may be compared with our $\Delta S$ value. However, the $\theta_D$ curve calculated by using the Shomate's results for $(NH_4)_2SO_4$ is superimposable on the $\theta_D$ curve for $(ND_4)_2SO_4$ by slight vertical displacement (Fig. 4), which fact strongly suggests that what is occurring in $(ND_4)_2SO_4$ is also occurring in $(NH_4)_2SO_4$ in the same way.

If we formally apply the Clapeyron-Clausius equation to the transition excluding the gradual part, we obtain a value of 0.33 cm$^3$ mol$^{-1}$ for the volume decrease from the low-temperature to the high-temperature phase by using the value[27] of $dT_c/dp = -4.0 \times 10^{-3}$ K kg$^{-1}$ cm$^2$. There is no other data to compare with this figure but the almost corresponding quantity[5] for $(NH_4)_2SO_4$ is 0.69 cm$^3$ mol$^{-1}$.

Now, we will consider the mechanism of the transition. From neutron diffraction studies,[9] there are two kinds of inequivalent ammonium ions, types I and II, in both phases, each of which changes the hydrogen bond arrangements as well as the extent of distortion from regular tetrahedral structure. The most eminent structural feature of the transition is the replacement of the mirror symmetry (the ab plane of the high-temperature phase) with the two-fold screw axis (low-temperature phase). O'Reilly and Tsang[20] developed a molecular field treatment of the transition using three-sublattice model on the basis of their experimental results of deuteron magnetic resonance[17]. The theory assumes essentially an order-disorder mechanism in which the two types of ammonium ions assume random distribution of two orientations separated by $\pm 30°$ from the mirror plane in the high-temperature phase. They also assumed that sulfate ions, which occupy the third sublattice, are also disordered in a similar manner. They derived two energy parameters $\varepsilon$ and $d\varepsilon/dn_\pm$ by fitting the theory to the temperature dependence of the crystal volume[5] in the low-temperature phase. Here $\varepsilon$ is the energy of a misoriented (antiparallel) pair relative to a parallel pair and $d\varepsilon/dn_\pm$ is its dependence on the number of the antiparallel pairs. The values they

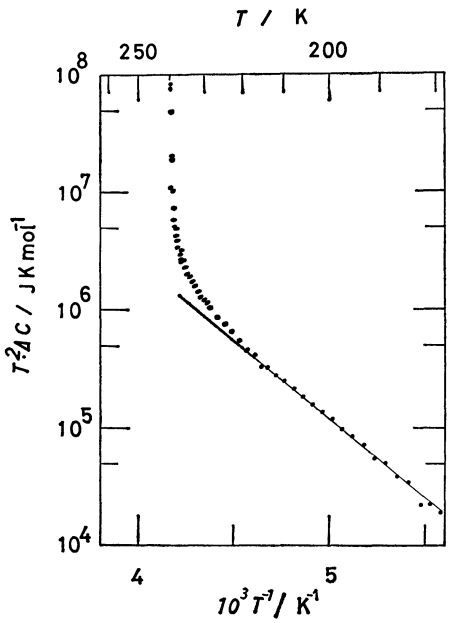


Fig. 8. Plot according to Eq. 1 for determination of enthalpy to form defects.

obtained were $\varepsilon = 0.92$ kJ mol$^{-1}$ and $d\varepsilon/dn_\pm = 0.10$ kJ mol$^{-1}$ for the case of six nearest neighbors.

The present thermodynamic results may be compared with the O'Reilly-Tsang theory in two ways. In the first place, the overall entropy of the transition is expected to be $\Delta S = 3R\ln 2 = 17.3$ J K$^{-1}$ mol$^{-1}$ according to the three-sublattice, order-disorder model in comparison with the experimental 20.4 J K$^{-1}$ mol$^{-1}$. The difference is outside of the experimental error; although there is small uncertainty in the evaluation of the 'normal' portion of the heat capacity, it can not account for the difference. Therefore, there must be some other small contributions to the entropy such as coupling of translational modes of motion with librational degrees of the ions.

The other quantity that can be compared with the theoretical model is the enthalpy to form a defect in the otherwise perfectly ordered structure. Suppose an ammonium ion is misoriented to create six 'wrong' pairs in the ordered lattice. This process requires an additional enthalpy of $6\varepsilon$ per ion. Since there are three such ions a formula unit, the total enthalpy per mole would be $h = 18\varepsilon$. Let $n$ be the number of such defects and the excess heat capacity due to this process of defect formation is given by

$$\Delta C_p = (\partial \Delta H/\partial T)_p = \partial(nh)/\partial T = (n_0 h^2/kT^2)\exp(-h/kT), \quad (1)$$

where the Boltzmann relation,

$$n = n_0 \exp(-h/kT),$$

has been used. Thus, a plot of $\ln(T^2\Delta C_p)$ *vs.* $T^{-1}$ should give a straight line whose slope yields a value of $h$. Figure 8 shows such a plot for $(ND_4)_2SO_4$ and the straight line corresponds to

$$n/N = 88 \exp(-1451/T),$$

which gives $h = 12.0$ kJ mol$^{-1}$ or $\varepsilon = 0.67$ kJ mol$^{-1}$. This is comparable in magnitude with 0.92 kJ mol$^{-1}$ which O'Reilly and Tsang derived. The observed

points in Fig. 8 begin to deviate from the straight line at about 173 K where the fraction of the defects reaches 2%. The deviation reflects the cooperative nature of the defect formation, in other words $h$ or $\varepsilon$ depends on the number of defects already present.

A similar analysis on the Shomate's data on $(NH_4)_2SO_4$ gave $h=12.2$ kJ mol$^{-1}$, indicating that one sees the same phenomenon in the two crystals.

An attempt to find the critical index was not successful because a plot of $\ln\Delta C_p$ against $\ln(T-T_c)/T_c$ did not give any straight line region.

In conclusion, the phase transition, whether ferroelectric or otherwise, in $(ND_4)_2SO_4$ consists of a second-order portion and a first-order portion, the former contributing 60% to the total entropy of transition. The thermal properties are consistent with the three-sublattice, order-disorder model proposed by O'Reilly and Tsang including disordering of the sulfate ions. It will help understand the mechanism better if the quadrupole effects of $^{17}O$ resonance may be studied in the two phases.

## References


1) J. L. Gronshaw and J. Ritter, *Z. Phys. Chem., B*, **16**, 143 (1932).
2) I. Nitta and K. Suenaga, *Bull. Chem. Soc. Jpn.*, **13**, 36 (1938).
3) C. H. Shomate, *J. Am. Chem. Soc.*, **67**, 1096 (1945).
4) B. T. Matthias and J. P. Remeika, *Phys. Rev.*, **103**, 262 (1956).
5) S. Hoshino, K. Vedam, Y. Okaya, and R. Pepinsky, *Phys. Rev.*, **112**, 405 (1958).
6) H. Ohshima and E. Nakamura, *J. Phys. Chem. Solids*, **27**, 481 (1966).
7) B. Singh, Dissertation, The Pennsylvania State University, 1962.
8) V. V. Vdalova and Z. G. Pinsker, *Soviet Phys.-Cryst.*, **8**, 433 (1964).
9) E. O. Schlemper and W. C. Hamilton, *J. Chem. Phys.*, **44**, 4498 (1966).
10) R. Blinc and I. Levstek, *J. Phys. Chem. Solids*, **12**, 295 (1960).
11) C. J. H. Schutte and A. M. Heyns, *J. Chem. Phys.*, **52**, 864 (1970).
12) B. H. Torrie, C. C. Lin, O. S. Binbrek, and A. Anderson, *J. Phys. Chem. Solids*, **33**, 697 (1972).
13) J. J. Rush and T. I. Taylor, Inelastic Scattering Neutrons Solids Liquids, Proc. Symposium, 3rd, Bombay, India, **2**, 333 (1965).
14) U. Dahlborg, K. E. Larsson, and E. Pirkmajer, *Physica*, **49**, 1 (1970).
15) R. E. Richards and T. Schaefer, *Trans. Faraday Soc.*, **57**, 210 (1961).
16) R. Miller, R. Blinc, M. Breuman, and J. S. Waugh, *Phys. Rev.*, **126**, 528 (1962).
17) D. E. O'Reilly and T. Tsang, *J. Chem. Phys.*, **46**, 1291 (1967).
18) R. R. Knispel, H. E. Petch, and M. M. Pintar, *J. Chem. Phys.*, **63**, 390 (1975).
19) D. W. Kydon, M. Pintar, and H. E. Petch, *J. Chem. Phys.*, **47**, 1185 (1967).
20) D. E. O'Reilly and T. Tsang, *J. Chem. Phys.*, **46**, 1301 (1967).
21) A. Onodera, H. Fujishita, and Y. Shiozaki, *Solid State Commun.*, **27**, 463 (1978).
22) P. Flubacher, A. J. Leadbetter, and J. A. Morrison, *Phil. Mag.*, **4**, 273 (1959).
23) J. L. Riddle, G. T. Furukawa, and H. H. Plumb, "Platinum Resistance Thermometry," NBS Monograph 126, 1973; *Metrologia*, **5**, 35 (1969).
24) Y. Higashigaki and H. Chihara, unpublished results.
25) Y. Higashigaki, Dissertation, Osaka University, 1977.
26) H. G. Unruh, *Solid State Commun.*, **8**, 1951 (1970).
27) S. Tsunekawa, Y. Ishibashi, and Y. Takagi, *J. Phys. Soc. Jpn.*, **33**, 862 (1972).